JOURNAL OF VIROLOGY, Jan. 1994, p. 366–378
0022-538X/94/$04.00+0

Vol. 68, No. 1

Retention by the Endoplasmic Reticulum of Rotavirus VP7 Is Controlled by Three Adjacent Amino-Terminal Residues

D. R. MAASS† AND P. H. ATKINSON*

Department of Developmental Biology and Cancer, Albert Einstein College of Medicine, Bronx, New York 10461

Received 28 May 1993/Accepted 8 October 1993

The rotavirus outer capsid glycoprotein, VP7, is an endoplasmic reticulum (ER) membrane-associated glycoprotein in both infected and transfected cells. It was previously demonstrated in this laboratory and by others that both the cleaved signal sequence (H2) and the first NH_2-terminal 61 amino acids of VP7 are sufficient and necessary for ER retention of this molecule. Using site-specific mutagenesis and transfection techniques, we show that residues Ile-9, Thr-10, and Gly-11 were specifically necessary for ER retention. These results further define the ER retention sequence of VP7 and demonstrate that conservative changes, apparently innocuous in only three adjacent amino acids, can lead to major solubility and compartmentalization changes. It was found that placement of the first 31 mature NH_2-terminal residues of VP7, in addition to the cleaved ER translocation signal sequence, was sufficient to retain the enzymatically active chimeric α-amylase in the ER; this enzyme is normally secreted. Deletions of the residues Ile-9, Thr-10, and Gly-11 within the amylase chimera containing 31 VP7 amino acids resulted in secretion of enzymatically active protein. It was also observed that the residues of VP7 presented in certain chimeras were able to abolish α-amylase enzymatic activity. These chimeras are presumably misfolded since it was demonstrated by pulse-chase experiments that these molecules are degraded in the ER. We surmise that a favorable conformation is necessary for retention since ER retention and activity of the chimeras depend on the primary sequence context.

The ability of the endoplasmic reticulum (ER) to retain its endogenous proteins while efficiently exporting proteins destined for the secretory pathway is fundamental to the proper function of the cell (27, 34). Motifs in the primary sequence within ER-resident proteins are involved in retaining these proteins in the ER (27, 34). These ER retention signals include the tetrapeptide Lys-Asp-Glu-Leu (KDEL; HDEL in yeast) at the COOH terminus of luminal ER proteins (23, 28), the presence of a highly charged cytoplasmic COOH terminus of ER transmembrane proteins, the presence of a consensus lysine three amino acids from the COOH terminus (10, 24, 26), and amino-terminal sequences of the ER-luminal protein of rotavirus (31, 32). It is now known that receptors exist in both mammalian and yeast cells which recognize KDEL (HDEL)-tailed proteins which may participate in the retrieval of ER proteins from a compartment distal to the ER (17, 18, 38, 48). Binding of the lysine-rich cytoplasmic tail of some ER transmembrane proteins to β-tubulin promotes polymerization to microtubulin (6). This specific association may prevent lateral movement of ER transmembrane proteins in the ER membrane and prevent their inclusion into transport vesicles (6).

The rotaviral outer capsid protein, VP7, is a membrane-associated ER glycoprotein in both infected and transfected cells (1, 8, 30, 32). The single open reading frame codes for 326 amino acids containing two hydrophobic domains of amino acids near the NH_2 terminus, each preceded by a methionine (3) (Fig. 1; H1 and H2). In vitro translation and in vivo transfection studies have shown that the first hydrophobic domain (H1) is not necessary for insertion into the ER and in most cases is probably not translated (32, 42, 49). The second hydrophobic domain (H2) is able to direct the protein into the ER and is cleaved, resulting in a glutamine at the mature NH_2 terminus (32, 42, 49). VP7 has properties characteristic of transmembrane proteins but lacks any obvious membrane anchor and is totally protected from exogenously added proteases (11, 42). VP7 contains a single N-linked glycosylation site, which is occupied by high-mannose carbohydrate primarily of the $Man_8GlcNAc_2$ species with some $Man_6GlcNAc_2$ seen, characteristic of ER glycoproteins (11). The processing of the VP7 carbohydrate is sensitive to temperature and energy blocks, although the ER mannosidase does not require energy, suggesting a transport step of VP7 to an ER subcompartment containing this processing enzyme (10a, 11).

The retention of VP7 in the ER has been the focus of numerous studies, including those from this laboratory. It was previously demonstrated in this laboratory and by others that the NH_2-terminal translated 82 amino acids of VP7, including the cleaved ER translocation signal sequence, are sufficient and necessary for ER retention of this molecule (31, 32, 40). It was first reported that the deletion of sequences within H2 and the mature NH_2 terminus (Δ−4–11) resulted in secretion of the mutated VP7 and the acquisition of carbohydrate resistant to the action of endo-β-N-acetylglucosaminidase-H (Endo H) showing transport to the Golgi apparatus (32). Evidence for the involvement of the translocation signal sequence (H2) for ER retention was shown by the secretion of VP7 which had its signal replaced by influenza virus hemagglutinin ER translocation signal, although the placement of the VP7 translocation signal onto a secretory protein did not result in ER retention, showing that H2 alone is not sufficient for ER retention (40). This suggests that a specific retention mechanism exists for retaining VP7 in the ER and that removal of this retention signal allows VP7 to enter into the secretory pathway and become secreted into the medium (32). The deletion of a retention signal of an ER resident protein will generally result in its inclusion into the secretory pathway if the mutated protein is not recognized as misfolded (27, 34). Properly folded structure (31, 51) clearly is a major question in studies of this

* Corresponding author. Mailing address: AgResearch, Wallaceville Animal Research Center, P.O. Box 40063, Upper Hutt, New Zealand. Phone: 64-4-528-6089. Fax: 64-4-528-6605.

† Present address: AgResearch, Wallaceville Animal Research Center, P.O. Box 40063, Upper Hutt, New Zealand.

FIG. 1. Single-letter code of the NH_2 terminus of VP7. The residue numbers indicate the position of the residue in the mature NH_2 terminus of processed VP7. H1 corresponds to the first hydrophobic domain (residues −45 to −28), whereas H2 corresponds to the second hydrophobic domain (residues −19 to −3). "Signal cleavage" indicates the site of processing by signal peptidase between Ala at −1 and Gln-1 to leave Gln-1 at the mature NH_2 terminus of VP7. CHO corresponds to the only N-linked glycosylation consensus sequence of VP7 at Asn-19. NcoI and BalI indicate the sites of these restriction endonucleases within the cDNA of the NH_2 terminus of VP7.

type, and we have approached the problem by use of an enzyme as the reporter protein when denatured chimeras display no enzymatic activity. We have used this approach previously by the construction of chimeras of VP7 with mature mouse salivary α-amylase (31). When the mature NH_2-terminal 61 residues of VP7 plus H2 were placed onto α-amylase, the chimera was retained in the ER in an enzymatically active form (31). It was therefore of interest to determine the minimum VP7 sequence required in the chimera for ER retention and to identify the NH_2-terminal residues within the minimum sequence that are essential for this retention.

In this study we used site-specific mutagenesis and transfection techniques to examine the NH_2-terminal ER retention signal of VP7 more closely. It was found that the residues Ile-9, Thr-10, and Gly-11 are essential amino acids of the VP7 ER retention signal and cannot be deleted or altered in maintenance of this function. The current studies also demonstrate that the minimum length of the mature NH_2 terminus of VP7 which is sufficient to retain α-amylase chimeras within the ER is 31 residues.

MATERIALS AND METHODS

Cells and antibodies. The simian virus 40-transformed Green monkey kidney cell line COS7 (9) was grown as monolayers in Dulbecco's modified Eagle's medium at 37°C. The growth medium was supplemented with 5% fetal bovine serum, 5% calf serum, 2 mM L-glutamine, 100 U of penicillin per ml, and 100 μg of streptomycin per ml (all from GIBCO Laboratories, Grand Island, N.Y.). Antisera used were (i) L56 and EJ, rabbit polyclonal antisera, raised against denatured SA11 VP7 purified from a sodium dodecyl sulfate (SDS)-polyacrylamide gel as described previously (32) and (ii) rabbit anti-human α-amylase antisera (Sigma Chemical Corp., St. Louis, Mo.).

Construction of VP7 deletions. All standard molecular biology procedures were performed as described by Maniatis et al. (22). All molecular biology reagents were from New England BioLabs, Inc., Beverly, Mass., except where noted. Oligonucleotides used were synthesized at the Albert Einstein College of Medicine oligonucleotide synthesis facility and are listed below.

PHA-1	AATACGACTCACTATAG	T7 promoter
PHA-4	GTGTTACTTCTGCTCT	simian virus 40 large T promoter
PHA-3	GCTAATTCAACGCAATGCCTATATTATCCG	Δ23–31
PHA-5	GAAGAAAGCTTCCTCGCTGCGAC	Δ28–38
PHA-6	TAAATCATTATCTAGAATA	*Xba*I-25
PHA-7	GGTATTAATCTTATGGACATTGCA	Δ8–12
PHA-12	AGAGCACAAAATTATATTGCATACGCT	Δ4–14
PHA-13	AGAGCACAAAATACAGGCTCCATG	Δ3–9
PHA-15	GGTATTAATCTTANAATCACAGGC	Pro-8 to Thr, Arg
PHA-16	GCACAAAATTATCTTCCAATG	Δ4–6
PHA-18	GGTATTAATCTTCCATCCATGGACATTGCA	Δ9–11
PHA-20	ATCACAGGCTCCATGTACGCTAATTCA	Δ14–16
PHA-21	GGTATTAATCTTATCACAGGCTCC	Δ8
PHA-22	GGTATTAATCTTGCAATCACAGGC	Pro-8 to Ala
PHA-27	ATTAATCTTCCAATCAG/AG/CGGCTCCATGGAGATT	Thr-10 to Ser, Asn, Lys
PHA-28	GGTATTAATCTTCCAAC/GGACAGGCTCCATGGAC	Ile-9 to Thr, Arg
PHA-29	AATCTTCCAATCACAGA/CCTCCATGGACATTGCA	Gly-11 to Ala, Asp
PHA-8	CGATCGATATCGTTTATTTC	$VP7_{45}$/amy
PHA-23	AACTGGCCAGTATGCAATGTCCATGGA	$VP7_{17}$/amy ± spacer
PHA-24	ACGTGGCCACGTTGAATTAGCGTATGC	$VP7_{21}$/amy ± spacer
PHA-25	TCGTGGCCAAAGTGTAGAAGTGAGGAA	$VP7_{31}$/amy ± spacer

The SA11 rotavirus VP7 coding sequence was excised from pJC9 (32) with *Xho*I, generating a 1,076-bp fragment. This purified fragment was ligated into pTZ19R (Pharmacia LKB Biotechnology, Uppsala, Sweden) at the *Sma*I site by using *Xho*I linkers, placing it under the control of the T7 promoter to generate VP7/pTZ19R. Deletion mutants Δ10–14, Δ13–16, and Δ45–61 were constructed by using *Bal* 31. VP7/pTZ19R was linearized with either *Nco*I or *Bal*I and digested with *Bal* 31, and the ends were made blunt with Klenow fragment. The *Bal*I-*Bal* 31-digested product was cut with *Eco*RI and treated with phosphatase, and the approximately 3,000- to 3,200-bp fragment was isolated. It was then ligated to the *Bal*I-*Eco*RI 713-bp fragment containing wild-type VP7 COOH terminus, generating various deletions from Trp-61 toward the NH_2 terminus. The same strategy was used to generate deletions of VP7 from Met-13 toward the COOH terminus. The *Nco*I-*Bal* 31-digested product was digested with *Pst*I and treated with phosphatase, and the approximately 3,400- to 3,680-bp fragment was isolated. It was ligated to the *Nco*I-*Pst*I 256-bp fragment in which the *Nco*I site was made blunt with Klenow fragment.

Oligonucleotide site-directed mutagenesis was performed by the procedure described by Kunkel (15) and Zoller and Smith (52) with oligonucleotide PHA6 for the construction of VP7-PHA6, generating an *Xba*I restriction site at leucine −25. Δ23–31, Δ28–38, Δ8–12, Δ4–14, Δ3–9, Δ4–6, Δ9–11, Δ8, and Δ14–16 were constructed with VP7/PHA6/pTZ19R as the template and the mutagenizing oligonucleotides listed above.

The resultant mutants were screened by chain-terminating sequencing incorporating ^{35}S-dATP (Amersham, Arlington Heights, Ill.) with either double-stranded or single-stranded DNA as the template (35). The wild-type sequence and the

in-frame deletion mutants were subcloned into the eucaryotic expression vector pJC119 by excising VP7 coding sequence from pTZ19R with *Cla*I and *Xho*I in conjunction with *Xho*I linkers (approximately 950 to 970 bp, containing only H2; termed dH1). The isolated fragments were cloned into the *Xho*I site in pJC119 (32).

PCR. Polymerase chain reaction (PCR) was performed with the GeneAmp DNA amplification reagent kit (Perkin Elmer Cetus, Norwalk, Conn.), using the manufacturer's procedures with the oligonucleotides listed above. The samples were incubated for 30 cycles consisting of a 2-min denaturation step at 94°C, a 2-min annealing step at 41°C, and a 3-min elongation step at 72°C. After completion, the products were phenol extracted and ethanol precipitated.

Construction of VP7/α-amylase chimeras. Salivary mouse α-amylase containing various lengths of the NH_2 terminus of VP7 was constructed as follows. The complete coding sequence of α-amylase (amy) was inserted into pJC119 (31). The resultant pJCAm was linearized with *Apa*I, blunted with T4 polymerase, and digested with *Xho*I to generate the coding sequence of mature α-amylase without its ER translocation signal sequence. The VP7 sequences to be inserted were generated by either PCR or oligonucleotide site-specific mutagenesis. $VP7_{24}$/dH1/amy/pJC119 was constructed by digesting Δ28–38/*Hin*dIII$_{24}$/dH1/pJC119 with *Hin*dIII and blunting the 5′ overhang with mung bean nuclease. After digestion with *Xho*I, the 180-bp fragment was isolated and ligated to amy/pJC119 lacking its signal sequence as described above. $VP7_{45}$/dH1/amy/pJC119 was constructed with the oligonucleotides PHA-1 (coding strand) and PHA-8 (complementary strand) in a PCR with VP7/pTZ19R as the template. The resulting 276-bp PCR fragment was digested with *Cla*I, *Xho*I linkers were ligated, and then the fragment was digested with *Eco*RV. The 246-bp fragment was isolated and ligated into amy/pJC119 lacking its signal. $VP7_{17}$/dH1/amy/pJC119, $VP7_{17+3}$/dH1/amy/pJC119, $VP7_{21+w}$/dH1/amy/pJC119, $VP7_{21+3}$/dH1amy/pJC119, $VP7_{31+}$/dH1/amy/pJC119, and $VP7_{31+3}$/dH1/amy/pJC119 were constructed with oligonucleotides listed above in PCRs with VP7/dH1/pJC119 as the template. The resultant fragments were digested with *Xho*I and were either cut with *Bal*I or untreated, and the isolated fragments were ligated into amy/pJC119 lacking its signal sequence.

Deletions within the VP7 61 NH_2-terminal residues were placed onto α-amylase by digesting the respective VP7 deletion, ΔVP7/dH1/pJC119, with *Bal*I and *Xho*I and ligating the purified fragments into amy/pJC119 lacking its signal sequence as described above. Deletions within the VP7 31 NH_2-terminal residues were generated by using the respective mutant template in a PCR with oligonucleotides PHA-4 and PHA-25. After digestion with *Xba*I, the fragments were ligated onto the mature NH_2 terminus of α-amylase as described above. All chimera junctions were confirmed by sequencing.

Transfection. Transfections were performed by electroporation as described previously (40). The transfected cells were plated onto a 100-mm dish containing 10 ml of growth medium and incubated at 37°C for 40 h. The cells were preincubated for 10 min at 37°C in methionine-deficient growth medium and then radiolabeled for 4 h in 1 ml of methionine-deficient growth medium to which 150 μCi of L-[^{35}S]methionine (Amersham) was added. Transfected cells treated with tunicamycin (Sigma) had 2 μg per ml added to the medium 2 h prior to and during radiolabeling. Pulse-chase experiments were performed by radiolabeling the transfected cell monolayers for 16 h at 37°C in 3.0 ml of reduced-methionine labeling medium (seven parts methionine-deficient labeling medium and three parts Dulbecco's modified Eagle's growth medium containing 10% heat-inactivated, dialyzed fetal calf serum) containing 50 μCi of L-[^{35}S]methionine (Amersham) per ml. Chases were initiated by replacing the labeling medium with growth medium and incubating at 37°C for the indicated times. Transfected cells treated with chloroquine had 100 μM chloroquine (Sigma) added 2 h prior to and during the chases. Transfected cells in which transport from the ER was blocked by low temperature (36, 45) were transferred to a 16°C water incubator during labeling chases. Cell lysates and media were immunoprecipitated and analyzed by SDS-polyacrylamide gel electrophoresis (PAGE) (9% polyacrylamide) (16) as previously described (32). Densitometry of fluorographs was performed by using an Ultrascan XL Laser densitometer (no. 2222-010; LKB Produkter Ab, Bromma, Sweden) in the linear range. Fluorographs of the same samples at lower and higher exposures were used to confirm peaks.

Amylase activity assay. Intracellular α-amylase activity was determined as described previously by method described by Bernfeld (2, 31). α-Amylase activity in transfected-cell medium was determined by immunoprecipitation from the medium in native conditions and performing the α-amylase assay on the protein A-Sepharose CL4B beads (Sigma). A 5.0-ml portion of medium was collected before radiolabeling, and nonadherent cells were centrifuged to a pellet in a microcentrifuge and discarded. Rabbit anti-human α-amylase antiserum (5.0 μl; Sigma) was added and incubated at 4°C for 16 h on a rocking platform. Protein A-Sepharose CL4B beads were added, and the mixture was incubated at 4°C for 3 h. The beads were collected by centrifugation, washed three times with 1% Nonidet P-40–0.15 M NaCl–0.05 M Tris-HCl (pH 7.5)–4 mM phenylmethylsulfonyl fluoride, and then resuspended in amylase dilution buffer. Aliquots of this suspension were used to measure α-amylase activity as described above.

Immunofluorescence localization. COS7 cells which had been transfected as described above were plated on glass coverslips (Corning Glass Works, Corning, N.Y.) and prepared for immunofluorescence as described previously (32) with the appropriate primary antibody.

In vitro transcription and translation. Transcription reactions were performed with the Riboprobe Gemini System (Promega, Madison, Wis.) as specified by the manufacturer. Translation reactions were performed as described previously with canine pancreas membranes and rabbit reticulocyte lysate as described (11, 29, 39). The samples were immunoprecipitated in the denatured state as described above.

RESULTS

Localization of VP7 ER retention signal. It was previously demonstrated in this laboratory that the 82 NH_2-terminal residues of VP7 are necessary and sufficient for its ER localization and retention (31, 32). Various deletions within the mature NH_2 terminus were constructed and transfected into COS7 cells to investigate which residues are essential for the ER retention of VP7. All the mutants in this study were derived from a wild-type cDNA of VP7 containing the coding sequence for only the second hydrophobic domain (Fig. 1), H2, a signal sequence cleaved by signal peptidase (32, 42). The nomenclature in this paper reflects this signal cleavage event in that the mature NH_2 terminus is assigned no. 1 and the signal sequence has negative numbers. The major initiation codon of VP7 is the methionine preceding H2 of the open reading frame; therefore, our mutants are designed with this knowledge (42).

Cells were transfected with the various mutant VP7s (Table 1) and expressed products tested for carbohydrate modifica-

TABLE 1. Summary of glycosylation and secretion of VP7 mutations

Deletion[a]	Glycosylation[b]	Secretion[c]
None	+	−
Δ−4–11	+	+
Δ45–61	±	−
Δ28–38	±	−
Δ25–61	±	−
Δ23–31	+	−
Δ3–9	+	+
Δ8–12	+	+
Δ10–14	+	+
Δ9–11	+	+
Δ4–6	±	−
Δ4–14	+	−
Δ14–16	+	−
Δ13–16	+	−
Δ8	+	−
Thr-8	++	+
Arg-8	+	−
Ala-8	+	−
Thr-9	+	+
Arg-9	+	−
Asn-10	++	+
Ser-10	+	+
Lys-10	+	+
Ala-11	+	+
Asp-11	+	+

[a] VP7 mutation where Δ indicates the inclusive residues deleted from VP7 and the three-letter amino acid code indicates the resultant amino acid replacing the wild-type residue.

[b] Glycosylation indicates the presence of N-linked glycosylation. Symbols: −, none; ±, incomplete; +, one site; ++, two sites.

[c] Secretion indicates whether a protein product was recovered in the medium. Symbols: +, recovered; −, not recovered.

tion by Golgi-specific processing enzymes (14). All the deletion mutants were expressed intracellularly, albeit at different levels, at their expected M_r, except for Δ3–9 which had a slower electrophoretic mobility (Fig. 2). The intracellular VP7 molecules were all glycosylated, with various efficiency, predominantly with the ER high-mannose (Endo H-sensitive) form (11, 43). For example, wild-type VP7, Δ−4–11, Δ3–9, Δ4–14, Δ8–12, Δ10–14, and Δ23–31 were fully glycosylated, whereas Δ25–61, Δ28–38, and Δ45–61 contained unglycosylated species (Fig. 2A), reflecting different efficiencies of oligosaccharyltransferase activity on mutant VP7s for unknown structural reasons. Deletion mutants Δ3–9, Δ8–12, and Δ10–14 resulted in VP7 molecules being secreted in an Endo H-resistant form (Fig. 2B) consistent with Golgi processing of the N-linked carbohydrate to complex forms. The medium of Δ10–14-transfected COS7 cells contained two immunoreactive products resistant to Endo H (Fig. 2B), perhaps reflecting differences in posttranslational modifications. Secreted Δ3–9 had a lower electrophoretic mobility than expected, mirroring its intracellular form. No protein products from deletions in the VP7 sequence beyond Glu-23 (Δ23–31, Δ25–61, Δ28–38, and Δ45–61) were secreted (Fig. 2B). Most of the total immunoreactive material of deletions that were secreted was found intracellularly after labeling for 4 h (Fig. 2), suggesting that release from the ER was rate limiting. One deletion mutant, Δ4–14, within the NH_2-terminal 14 residues did not result in secretion, although it lacks the majority of this domain and was found only as an Endo H-sensitive intracellular form (Fig. 2).

It was concluded that the VP7 retention signal resides in the first 23 NH_2-terminal residues. For nonsecreted deletion mutants, it cannot be ruled out that they were retained because of misfolding.

Other deletions in the NH_2 terminus of VP7 were examined, to further probe the sequences necessary for retention and to examine this region more closely (Fig. 3A). The only mutant

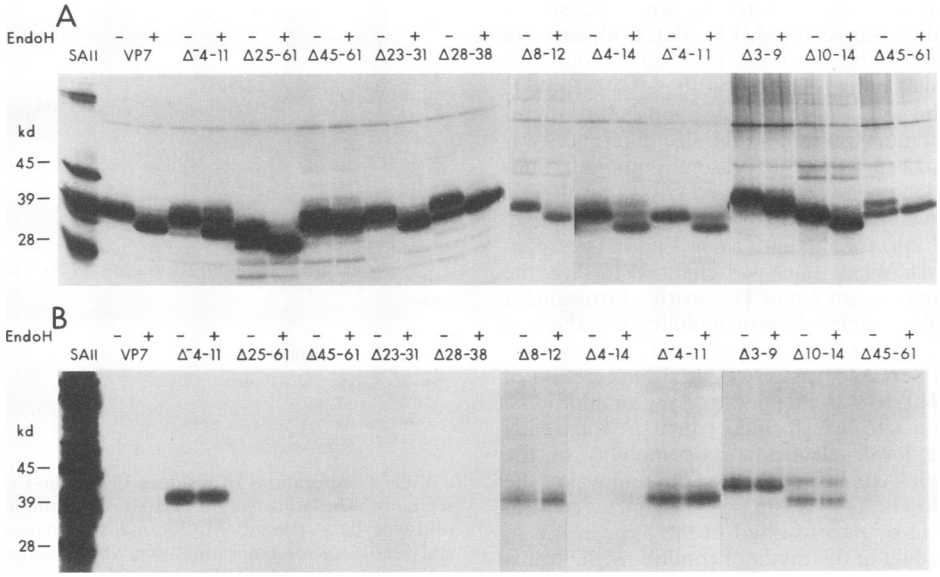

FIG. 2. Only deletions within the first 14 residues of the mature NH_2 terminus of VP7 result in secretion. Plasmids encoding deletion mutants of VP7, where Δ indicates the inclusive residues removed, under the control of the simian virus 40 late promoter were electroporated into COS7 cells. The transfected cells were metabolically labeled, and lysates and medium were immunoprecipitated with anti-VP7 antiserum. Immunoprecipitated products were treated in the presence or absence of Endo H and analyzed on reducing SDS-PAGE (11% polyacrylamide). (A) Intracellular. (B) Medium. SA11 corresponds to SA11 rotavirus-infected MA104 cell lysate used for molecular mass markers. Molecular masses correspond to VP6 (45 kDa), VP7 (39 kDa), and NS28 (28 kDa).

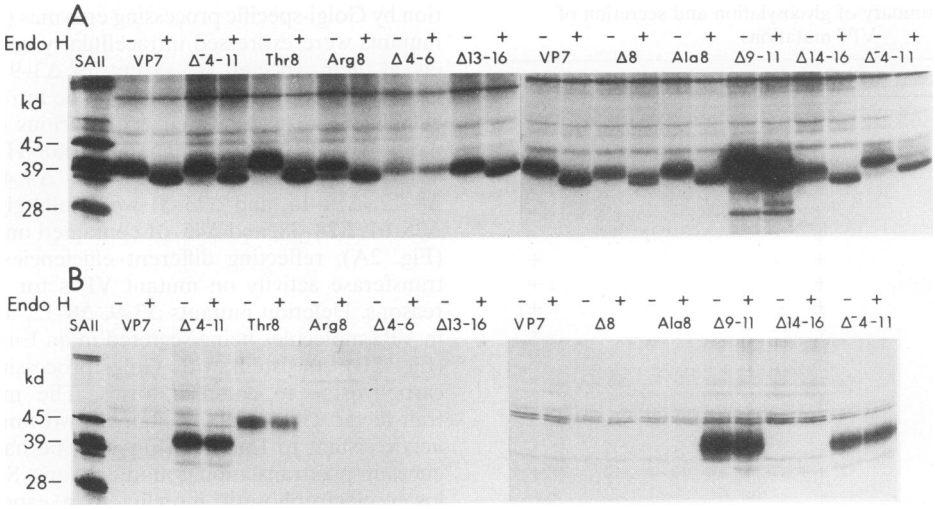

FIG. 3. Absence of residues Ile-9, Thr-10, and Gly-11 or addition of an N-linked glycosylation at Asn-6 results in secretion. Thr8, Arg8, and Ala8 indicate point mutations which change the wild-type Pro at residue 8 to the indicated amino acid. In vivo expressed products were detected as in Fig. 2. (A) Intracellular. (B) Medium. SA11 corresponds to SA11 rotavirus-infected MA104 cell lysate used for molecular mass markers. Molecular masses correspond to VP6 (45 kDa), VP7 (39 kDa), and NS28 (28 kDa).

product secreted was Δ9–11, which was Endo H resistant (Fig. 3B). The protein products of small deletions neighboring residues 9–11, i.e., Δ4–6, Δ8, Δ13–16, and Δ14–16, were not detected in the media (Fig. 3B), which, taken with the results shown in Fig. 2, begin to delineate finely the NH_2-terminal region of VP7 necessary for ER retention.

Point mutations were introduced into the VP7 sequence in this region. The replacement of Pro-8 with Ala or Arg did not result in the appearance of the mutant product in the medium (denoted Ala-8 and Arg-8; Fig. 3). When Pro-8 was changed to Thr, it generated an additional N-linked glycosylation consensus sequence at Asn-6, in addition to the wild-type site at Asn-19, and the product was secreted (Fig. 3B). Both sites are apparently used as seen in the lower electrophoretic mobility in the Thr-8–Endo H lane compared with wild-type VP7–Endo H sample (Fig. 3A). This size difference was abolished on treatment with Endo H, demonstrating that the size differences was due entirely to the extra carbohydrate present. Point mutations in the tripeptide sequence Ile-9, Thr-10, and Gly-11 resulted in secretion of the molecule. Alteration of Ile-9 to Thr resulted in the secretion of VP7 into the medium as an Endo H-resistant species (Thr-9, Fig. 4). When Ile-9 was changed to Arg, the product was found only as an Endo H-sensitive intracellular species that had a higher electrophoretic mobility than those of species with the other point mutations (Fig. 4). The replacement of Thr-10 with Ser, Asn, or Lys resulted in secretion of the variants. When Thr-10 was changed to Asn, an additional N-linked glycosylation site was formed which is apparently used as seen in the lower electrophoretic mobility of the intracellular form, which can be reversed by the removal of the carbohydrate by Endo H (Asn-10, Fig. 4). The replacement of Gly-11 with either Ala or Asp resulted in the appearance of Endo H-resistant product in the medium containing the transfected cells (Fig. 4). The intracellular product of Lys-11 had a lower electrophoretic mobility than expected, and its secreted product displayed several immunoreactive bands. It is not known whether the replacements within the mainly hydrophobic domain of the NH_2 terminus with polar or charged residues or whether other unknown modifications account for this altered mobility since VP7 displays anomolous migration on SDS-PAGE.

We conclude that the three residues Ile-9, Thr-10, and Gly-11 are essential for the retention of VP7 in the ER. Changes to Pro-8, which might be expected to play a role in protein folding, made no difference.

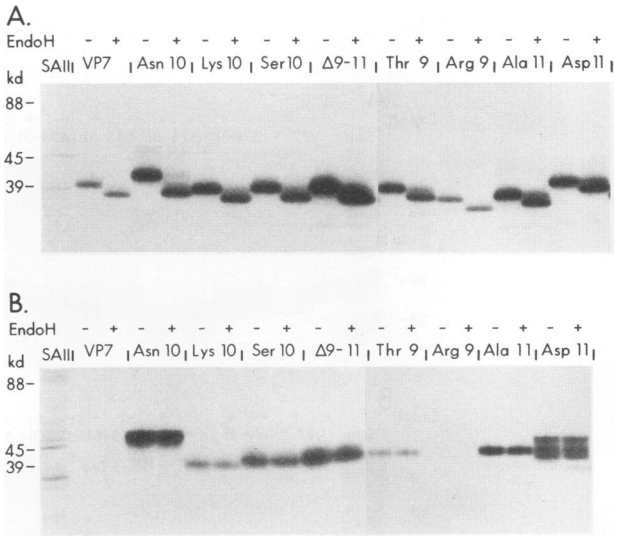

FIG. 4. Alterations of residues Ile-9, Thr-10, and Gly-11 result in secretion. Thr9 and Arg9 indicate point mutations which change the wild-type Ile at residue 9 to the indicated amino acid. Asn10, Lys10, and Ser10 indicate point mutations which change the wild-type Thr at residue 10 to the indicated amino acid. Ala11 and Asp11 indicate point mutations which change the wild-type Gly at residue 11 to the indicated amino acid. In vivo expressed products were detected as in Fig. 2. (A) Intracellular. (B) Medium. SA11 corresponds to SA11 rotavirus-infected MA104 cell lysate used for molecular mass markers. Molecular masses correspond to VP4 (88 kDa), VP6 (45 kDa), and VP7 (39 kDa).

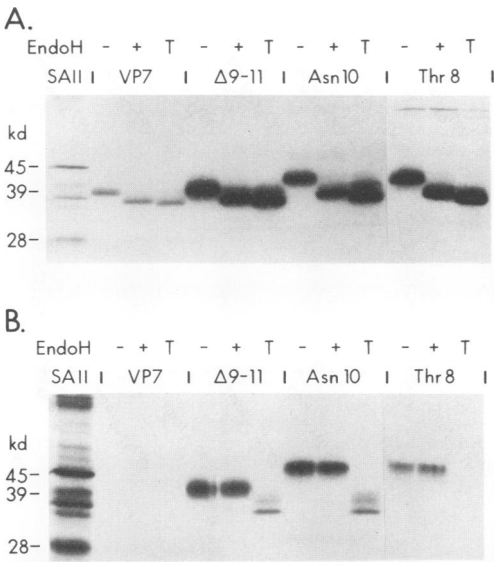

FIG. 5. Inhibition of glycosylation abolishes the secretion of Thr-8 but not the secretion of Asn-10. COS7 cells were electroporated with the corresponding cDNAs and treated in the presence or absence of tunicamycin 6 h before and during metabolic labeling. Products were detected and analyzed as in Fig. 2, except that no Endo H treatment was performed on the tunicamycin-treated samples (lanes T). (A) Intracellular. (B) Medium. SA11 corresponds to SA11 rotavirus-infected MA104 cell lysate used for molecular mass markers. Molecular masses correspond to VP6 (45 kDa), VP7 (39 kDa), and NS28 (28 kDa).

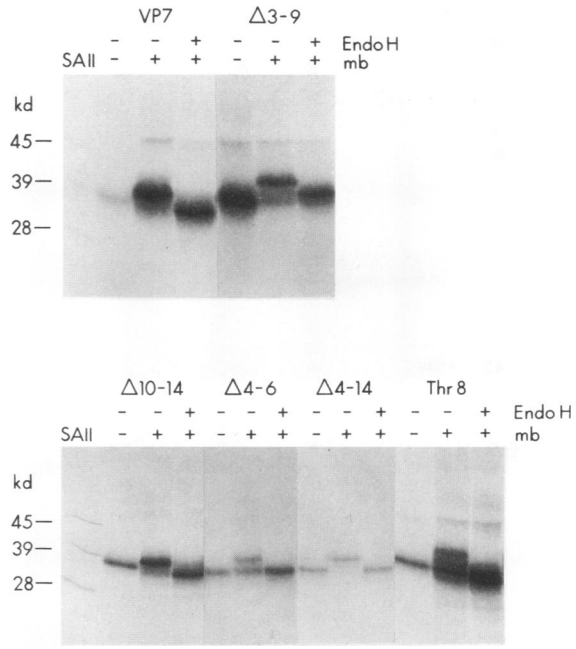

FIG. 6. The presence of the translocation signal (H2) of VP7 is not sufficient for ER retention. Determination of signal cleavage of VP7 mutants was performed by in vitro translation of VP7 mutant transcripts in the presence or absence of microsomal membranes (mb). Products were immunoprecipitated with anti-VP7 antiserum, treated in the presence or absence of Endo H, and analyzed by reducing SDS-PAGE (11% polyacrylamide). The immunoreactive products in the presence of microsomes were protected from exogenously added proteases.

The involvement of the extra carbohydrates in the secretion of Thr-8 and Asn-10 was examined by treating the transfected COS7 with tunicamycin, an N-linked glycosylation inhibitor (47). Wild-type VP7 is still retained in the ER, and Δ9–11 secretion is unaffected in the presence of tunicamycin (Fig. 5). This demonstrates that the N-linked glycosylation at Asn-19 does not contribute to the retention of wild-type VP7 in the ER or to secretion of Δ9–11. When Thr-10 is changed to Asn-10, an unglycosylated protein is secreted in the presence of tunicamycin, indicating that the point mutation changing Thr-10, and not the concomitant glycosylation, was responsible for its secretion. In contrast, the medium of cells transfected with Pro-8 changed to Thr-8 and treated with tunicamycin did not display any appreciable amount of secreted VP7 (Fig. 5), suggesting that the additional carbohydrate in the Thr-8 mutant may decrease the hydrophobicity of the NH_2 terminus, allowing for secretion. Thus the actual Pro-8 to Thr-8 point mutation has no role in the retention of VP7 in the ER, and Thr-10 is essential for VP7 retention.

Role of signal cleavage in retention of VP7 in the ER. It has been demonstrated that the translocation signal sequence of VP7 (H2) is cleaved, leaving Gln-1 as the mature NH_2 terminus (42). It also has been reported that the H2 domain was necessary for the retention of VP7 in the ER, even though it is cleaved (40). Previous investigations by this laboratory demonstrated that Δ − 4–11 has its signal cleaved, although the precise site is unknown since the deletion removes the normally used cleavage site (32). It was also shown that H2 of the deletion mutant Δ1–11 was not processed and this mutant was retained in the ER (32). Thus, it was of interest to determine whether signal cleavage occurred in the deletion and point mutants generated in this study. The M_r of the in vitro protein product of mRNA translated in the presence of microsomes and digested with Endo H, compared with that of the primary translation product, demonstrates a shift in the M_r of the protein, indicative of the removal of the H2 domain. This size difference is evident in wild-type VP7, Δ10–14, and Thr-8, suggesting that signal cleavage occurred in these proteins (Fig. 6). This size change is not seen for Δ3–9, a deletion mutant which is secreted, indicating that the H2 domain is still present. This demonstrates that the presence of the H2 domain is not sufficient for ER retention and that this signal sequence does not anchor the protein in the membrane, since the product can be recovered in the medium of transfected cells (Fig. 2). The presence of this hydrophobic stretch in the context of this deletion is not recognized as a misfolded protein, since it is able to enter the secretion pathway (7, 21). It was also observed that no size change was evident for the Δ4–6 and Δ4–14 deletion mutants (Fig. 6), indicating a lack of signal cleavage for these proteins. It is not known whether the presence of the signal sequences in these mutants causes misfolding, thus retaining these mutants in the ER, or whether the residues essential for ER retention were still present in these VP7 deletion mutants.

ER retention requirements of VP7/α-amylase chimeras. It is clear that the presence of Ile-9, Thr-10, and Gly-11 is required for the retention of VP7 in the ER, although the context in which these residues appear is important in their function as an ER retention signal. This context dependence was examined by constructing chimeric molecules having various lengths of the NH_2 terminus of VP7 placed on salivary mouse α-amylase, a normally secreted protein. Either 24 or 45 residues of the mature NH_2 terminus of VP7 plus the H2 domain was placed

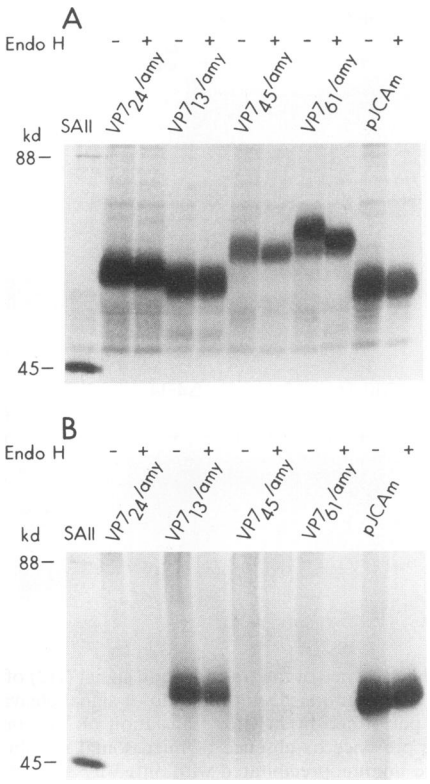

FIG. 7. Additional NH_2-terminal residues of VP7 are required to retain an α-amylase chimera. Corresponding cDNAs, where the subscripts indicate the number of residues of the NH_2 terminus of VP7 attached to α-amylase and pJCAm is wild-type α-amylase, were electroporated into COS7 cells. The transfected monolayers were metabolically labeled, and the lysates and medium were immunoprecipitated with anti-α-amylase antiserum and treated in the presence or absence of Endo H. Immunoprecipitated products were analyzed by reducing SDS-PAGE (9% polyacrylamide). (A) Intracellular. (B) Medium. SA11 corresponds to SA11 rotavirus-infected MA104 cell lysate used for molecular mass markers. Molecular masses correspond to VP4 (88 kDa) and VP6 (45 kDa).

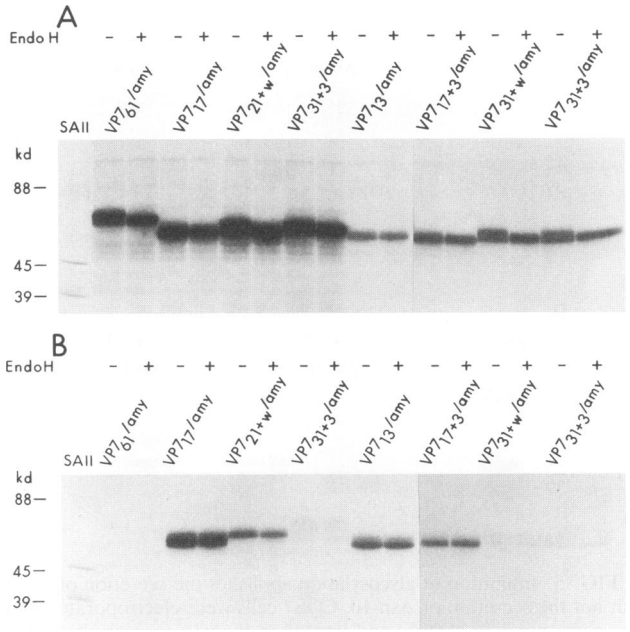

FIG. 8. The minimum context in which Ile-9, Thr-10, and Gly-11 can function in ER retention is 31 NH_2-terminal residues of VP7. Corresponding cDNAs were electroporated into COS7 cells, where +w indicates a Trp placed at the junction of the NH_2-terminal sequences of VP7 and α-amylase whereas +3 indicates Trp, Pro, Arg placed at the junction of the chimera. The products were detected as in Fig. 7 and analyzed by reducing SDS-PAGE (9% polyacrylamide). (A) Intracellular. (B) Medium. SA11 corresponds to SA11 rotavirus-infected MA104 cell lysate used for molecular mass markers. Molecular masses correspond to VP4 (88 kDa), VP6 (45 kDa), and VP7 (39 kDa).

onto mature mouse salivary α-amylase and expressed in transfected cells (Fig. 7). As seen previously, the addition of the 61 NH_2-terminal residues of VP7 to mature α-amylase resulted in only intracellular material containing Endo H-sensitive carbohydrate, indicative of the high-mannose structure found in the ER (31). Placement of a VP7 NH_2 terminus of only 13 residues was not sufficient for retention (31). Both $VP7_{24}$/amy and $VP7_{45}$/amy were retained intracellularly with no secreted material detected (Fig. 7). $VP7_{45}$/amy was partially glycosylated with an Endo H-sensitive carbohydrate, whereas $VP7_{24}$/amy did not appear to be glycosylated, even though it contained the N-linked glycosylation sequence of VP7 (Fig. 7). Lack of glycosylation of $VP7_{24}$/amy was demonstrated by the lack of an M_r shift of the chimeras in transfected cells in the presence or absence of tunicamycin (data not shown).

NH_2-terminal sequences of VP7 17, 21, or 31 residues in length (excluding small spacers) on α-amylase were generated to test the effect of the length of VP7 on glycosylation and presumably protein folding in the chimeras and were expressed (Fig. 8). The $VP7_{21}$/amy and $VP7_{31}$/amy chimeras contained Endo H-sensitive carbohydrate intracellularly (Fig. 8). The $VP7_{17}$/amy chimera was not glycosylated since it lacked the VP7 glycosylation consensus sequence at Asn-19. (Fig. 8). The placement of 21 residues of VP7 on α-amylase was not sufficient to retain the chimera in the ER, since molecules containing Endo H-resistant carbohydrate were secreted, consistent with passage through the Golgi and processing to complex forms (Fig. 8B). Chimeric molecules containing 17 residues of VP7 were also seen in the medium of transfected cells, indicating secretion of these molecules. This was in contrast to the $VP7_{31}$/amy chimera, in which no detectable material was secreted (Fig. 8B). Densitometry of the immunoprecipitated intracellular material and products from the medium demonstrated that the ratio of secreted to total cellular immunoreactive material was lower for $VP7_{21}$/amy than for $VP7_{17}$/amy, with no secretion seen for $VP7_{31}$/amy (data not shown).

Protein folding of the α-amylase catalytic domain was determined by assaying for the presence of α-amylase activity on a starch substrate in transfected-cell lysates (2, 31). These VP7/amy chimeras had α-amylase enzymatic activity comparable to or above levels found in α-amylase-transfected cells, except for the chimera $VP7_{24}$/amy, which had the same activity as untransfected cell lysate (Table 2) and was therefore probably denatured.

Secreted α-amylase activity was measured by performing the assay on immunoprecipitated material bound to protein A-Sepharose CL4B beads to obtain above-background values. The medium of α-amylase- and $VP7_{13}$/amy-transfected cells revealed α-amylase activity, which was not the case in the medium of chimeras which were retained intracellularly,

TABLE 2. Summary of glycosylation, secretion, and α-amylase activity of VP7/α-amylase chimeras

Chimera[a]	Glycosylation[b]	Secretion[c]	Intracellular activity[d]
pJCAm	−	+	+
$VP7_{61}$/amy	+	−	++
$VP7_{45}$/amy	+	−	+
$VP7_{31}$/amy	±	−	+
$VP7_{24}$/amy	−	−	−
$VP7_{21}$/amy	+	+	+
$VP7_{17}$/amy	−	+	+/−
$VP7_{13}$/amy	−	+	+
$\Delta-4–11_{61}$/amy	+	+	++
$\Delta8–12_{61}$/amy	+	−	++
$\Delta3–9_{61}$/amy	+	+	++
$\Delta4–14_{61}$/amy	+	+	+
$\Delta13–16_{61}$/amy	+	−	+
$\Delta10–14_{61}$/amy	+	−	++
$\Delta28–38_{61}$/amy	−	−	−
Thr-8_{61}/amy	++	−	+
Arg-8_{61}/amy	+	−	+
$\Delta-4–11_{31}$/amy	+	+	+
$\Delta3–9_{31}$/amy	+	+	+
$\Delta4–14_{31}$/amy	+	+	+
$\Delta8–12_{31}$/amy	+	+	+
$\Delta14–16_{31}$/amy	+	+	+
$\Delta9–11_{31}$/amy	+	+	+
Thr-8_{31}/amy	++	+	+

[a] The subscripts indicate the number of residues from the NH_2 terminus of VP7 placed onto α-amylase, the Δ indicates the inclusive residues deleted from VP7 NH_2-terminal sequence, +W indicates a Trp placed at the junction of the VP7 NH_2-terminal sequences and α-amylase, and +3 indicates Trp, Pro, Arg placed at the junction of the chimera.

[b] Glycosylation indicates the presence of N-linked glycosylation. Symbols: −, none; ±, incomplete; +, one site; ++, two sites.

[c] Secretion indicates whether the protein product was recovered in the medium. Symbols: +, recovered; −, not recovered.

[d] Intracellular activity indicates the presence of α-amylase activity in the transfected intracellular lysates. Symbols: +, activity comparable to α-amylase; ++, activity significantly above α-amylase; ±, is activity significantly below α-amylase; −, activity comparable to untransfected cells. Enzymatic activity was found in the medium of cells transfected with pJCAm, $VP7_{13}$/amy, and $\Delta-4–11_{61}$/amy, whereas no α-amylase activity was detected in the medium of cells transfected with $VP7_{61}$/amy or $VP7_{45}$/amy.

$VP7_{61}$/amy and $VP7_{45}$/amy (Table 2). This suggests that in addition to proper folding of the α-amylase catalytic domain in the secreted proteins, the overall chimeric molecule is not recognized as a misfolded protein.

It is concluded that at least 31 residues of the VP7 NH_2-terminal sequence is sufficient to retain α-amylase, a normally secreted molecule, within the ER. Also, the addition of VP7 sequences to the NH_2 terminus of α-amylase does not perturb the catalytic domain, except for the chimera $VP7_{24}$/amy, which has two charged amino acids abutting the amylase NH_2 terminus.

Mutants with deletion mutations in the VP7/α-amylase chimeras. When the deletion within VP7, $\Delta-4–11$, which results in secretion of VP7, was introduced into the $VP7_{61}$/amy chimera, it resulted in the secretion of the resultant mutant chimera, $\Delta-4–11_{61}$/amy (32). Various deletions and point mutations of the VP7 NH_2 terminus were introduced into the $VP7_{61}$/amy chimera and expressed to test for the ability of the mutants to allow secretion (Fig. 9). A VP7 deletion mutant, Δ3–9, that resulted in secretion of VP7 also resulted in secretion when introduced into the $VP7_{61}$/amy chimera $\Delta3–9_{61}$/amy (Fig. 9B). Mutants which were retained intracellularly when present in VP7 were also retained intracellularly when presented as an α-amylase chimera (Fig. 9, $\Delta13–16_{61}$/amy, $\Delta28–38_{61}$/amy, Arg8_{61}/amy). These chimeras were glycosylated with Endo H-sensitive carbohydrate, except for $\Delta28–38_{61}$/amy, which was unglycosylated. α-Amylase activity was determined to be present in the cell lysates expressing these chimeras, except for the $\Delta28–38_{61}$/amy chimera (Table 2), which, besides being unglycosylated, was inactive. Unexpectedly, other mutations which resulted in VP7 secretion, Thr-8 (mutated from Pro-8), Δ10–14, and Δ8–12, did not result in secreted products when introduced into the $VP7_{61}$/amy chimera (Fig. 9). These chimeras contained Endo H-sensitive carbohydrate intracellularly, and the size difference of Thr-8_{61}/amy between samples containing and lacking Endo H suggested that both glycosylation sites, Asn-6 and Asn-19, were used. It is unknown why these chimeras were retained, since they possessed α-amylase activity comparable to that of the $VP7_{61}$/amy chimera (Table 2), indicating that the catalytic domain was folded properly, although it is unknown whether the VP7 portion of the chimera was folded properly. A mutant, Δ4–14, which was retained intracellularly as a VP7 deletion, was recovered in the medium as an Endo H-resistant form when placed in a chimera with a 61-mer VP7, $\Delta4–14_{61}$/amy (Fig. 9B). Taken together, these inexplicable results led to a reexamination of whether a 61-amino-acid contribution of VP7 represented a valid context for deletion analysis.

As a result, various deletions and point mutations were examined in a smaller VP7 context, namely a 31-amino-acid VP7 NH_2-terminal sequence ($VP7_{31}$/amy) chimera to determine whether these chimeras had the same secretion phenotype as the alterations had in VP7. The chimeras Thr-8_{31}/amy and $\Delta8–12_{31}$/amy were secreted in the medium as an Endo H-resistant form (Fig. 10). These alterations were found to result in the secretion of VP7 but did not cause secretion when placed in the context of $VP7_{61}$/amy chimeras. The chimera $\Delta9–11_{31}$/amy was secreted, indicating that these residues are essential for the retention of the α-amylase chimeras in the ER (Fig. 10). The chimera $\Delta4–14_{31}$/amy was secreted, although it is not known whether the secretion is due to the deletion or to the shortened VP7 NH_2 terminus of the $VP7_{31}$/α-amylase chimera. A VP7 deletion mutant, Δ14–16, that was retained was also found to be retained when in the context of the $VP7_{31}$/amy chimera, although it was only partially glycosylated (Fig. 10). All these chimeras had α-amylase enzymatic activity comparable to that of the $VP7_{31}$/amy chimeras (Table 2), indicating the α-amylase catalytic domain was properly folded.

It was concluded that the $VP7_{31}$/amy chimeras contained the VP7 ER retention signal and that alterations in these chimeras had the same secretion phenotype as the alterations had in VP7 alone. In contrast, it was observed that larger deletions of the VP7 ER retention signal were required in the context of the $VP7_{61}$/amy chimeras than in VP7 alone or in the $VP7_{31}$/amy chimeras to allow for the secretion of the various mutant molecules. Implications of VP7 context in chimeras are discussed below.

Degradation of VP7/α-amylase chimeras. There is evidence of a proteolytic degradative pathway resident in the ER, apparently for molecules which are misfolded or fail to achieve their correct polymeric structure (13). It was of interest to determine the fate of the enzymatically inactive VP7-amylase chimeras in this context. Pulse-chase experiments were performed to determine the kinetics of degradation of chimeras which were retained in the ER to gain insight into chimeric protein folding. All the chimeras were expressed and were retained intracellularly for at least 6 h, except for the enzymatically inactive chimeras $VP7_{24}$/amy and $\Delta28–38_{61}$/amy, whose presence was greatly diminished after a 1-h chase (Fig. 11).

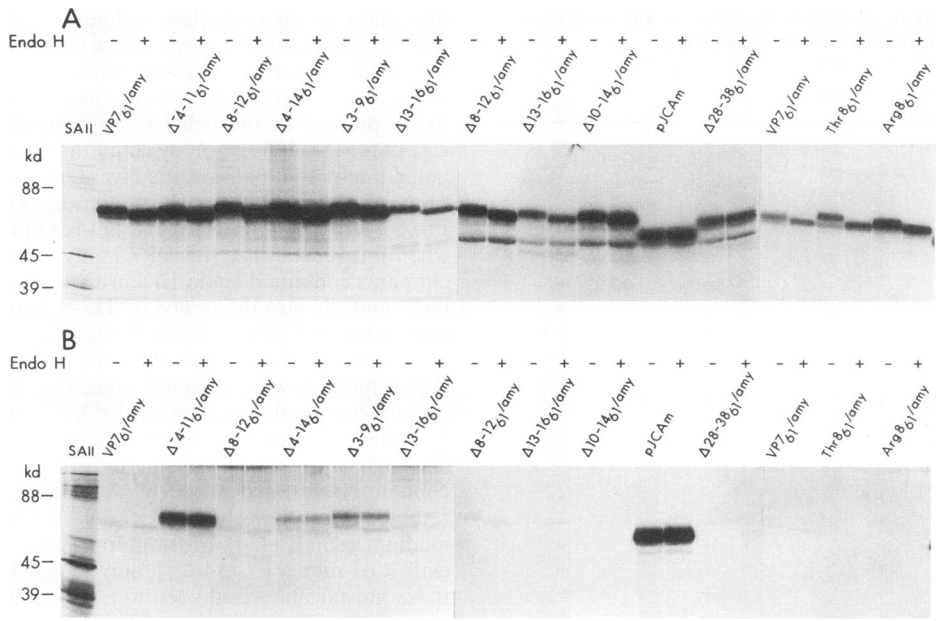

FIG. 9. VP7 alterations in the context of VP7$_{61}$/α-amylase chimeras do not mirror VP7 deletion secretion phenotypes. Corresponding cDNAs, where the Δ indicates the inclusive residues deleted from the NH_2-teminal sequence of VP7 and Thr8 and Arg8 indicate point mutations which change the wild-type Pro at residue 8 to the indicated amino acid, were electroporated into COS7 cells. The products were detected as in Fig. 7 and analyzed by reducing SDS-PAGE (9% polyacrylamide). (A) Intracellular. (B) Medium. SA11 corresponds to SA11 rotavirus-infected MA104 cell lysate used for molecular mass markers. Molecular masses correspond to VP4 (88 kDa), VP6 (45 kDa), and VP7 (39 kDa).

The enzymatically active chimeras, VP7$_{61}$/amy, Δ8–12$_{61}$/amy, and Δ13–16$_{61}$/amy (Table 2), were relatively undegraded (Fig. 11). ER degradation provides further evidence that proper protein folding probably is not achieved in VP7$_{24}$/amy and Δ28–38$_{61}$/amy chimeras and that the degradation assay monitors proper protein folding, as does the above-described assay of α-amylase enzymatic activity.

To further support this conclusion, the intracellular location of degradation of enzymatically inactive VP7$_{24}$/amy chimeras was investigated by using either a temperature treatment known to block exit from the ER (36, 45) or treatment with chloroquine, an agent which inactivates lysosomal proteases by increasing the intracellular pH (25, 50). The addition of chloroquine had no effect on VP7$_{24}$/amy degradation, since less than 20% was remaining after a 1-h chase, which mirrored the kinetics of degradation of the chimeras from the untreated transfected cells. A block in transport from the ER imposed by incubation of the transfected cells at 16°C (36, 45) inhibited the degradation of VP7$_{24}$/amy (Fig. 12), underscoring that the proteolysis was within the ER.

Indirect immunofluorescence was performed for intracellular localization of VP7$_{24}$/amy, since there was no carbohydrate available to use as a processing marker. Indirect immunofluorescence of permeabilized transfected COS7 cells with α-amylase antisera and fluorescein-conjugated immunoglobulin G secondary antibody was compared with the localization of the Golgi marker, rhodamine-conjugated wheat germ agglutinin, which binds to sialic acid and terminal glucosamines (46). Wild-type VP7, VP7$_{61}$/amy, and VP7$_{24}$/amy yielded a distinct and reticular pattern which was concentrated near the nucleus but also extended toward the periphery of the cell in addition to a perinuclear staining (Fig. 13a, c, and e). The staining of VP7 and the VP7/amy chimeras was distinct from that seen for the rhodamine-conjugated wheat germ agglutin, which yielded a punctate perinuclear localization (Fig. 13b, d, and f). The

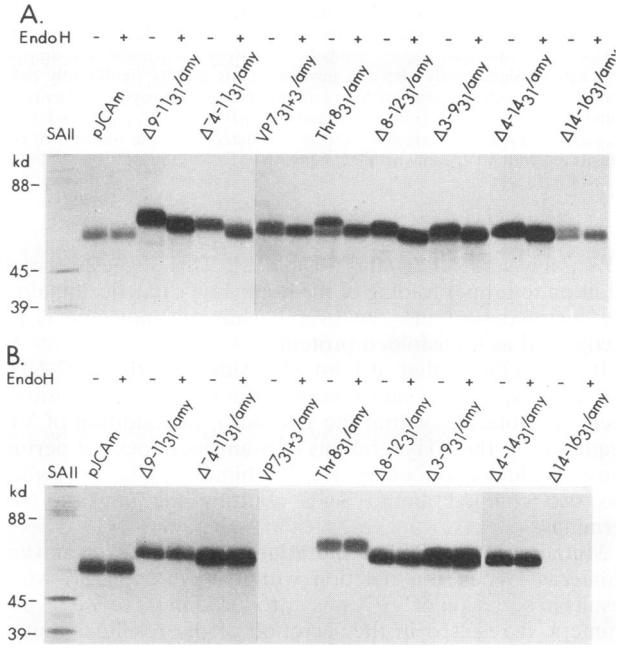

FIG. 10. VP7 alterations in the context of VP7$_{31}$/α-amylase chimeras mirror the VP7 deletion secretion phenotype. Corresponding cDNAs were electroporated into COS7 cells, and products were detected as in Fig. 7 and analyzed by reducing SDS-PAGE (9% polyacrylamide). (A) Intracellular. (B) Medium. SA11 corresponds to SA11 rotavirus-infected MA104 cell lysate used for molecular mass markers. Molecular masses correspond to VP4 (88 kDa), VP6 (45 kDa), and VP7 (39 kDa).

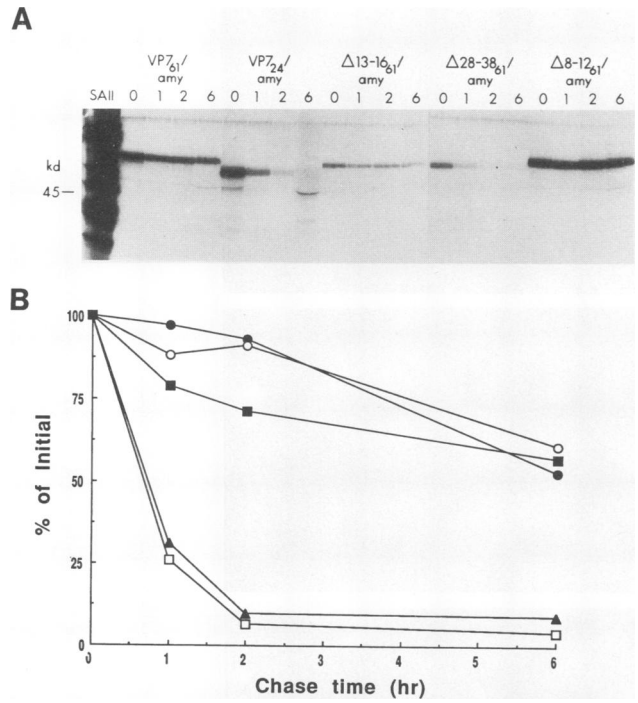

FIG. 11. Enzymatically inactive VP7/α-amylase chimeras are rapidly degraded intracellularly. COS7 cells were electroporated with the corresponding cDNAs, metabolically labeled to steady-state conditions, and chased for various times in the presence of excess methionine and cysteine. Cell lysates were immunoprecipitated with anti-α-amylase antiserum, and the products were analyzed by reducing SDS-PAGE (9% polyacrylamide). SA11 corresponds to SA11 rotavirus-infected MA104 cell lysate used for molecular mass markers. Molecular mass corresponds to VP6 (45 kDa). (B) Graph of the degradation rate. Chimeric bands were normalized to total protein present by densitometric comparison with an apparently undegraded background band near the top of the gel.

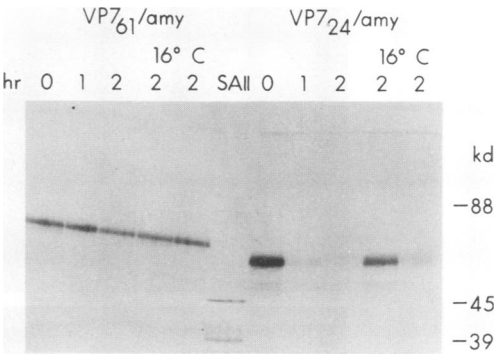

FIG. 12. Degradation of the VP7$_{24}$/α-amylase chimera occurs in the ER. VP7$_{61}$/amy and VP7$_{24}$/amy cDNAs were electroporated into COS7 cells, and their products were metabolically labeled as in Fig. 11, except that chases were performed for 1 h (lanes 1), 2 h (lanes 2), in the presence of chloroquine for 2 h (lanes C), or with an incubation temperature of 16°C for 2 h (lanes 16°). Immunoprecipitated products were analyzed by reducing SDS-PAGE (9% polyacrylamide). SA11 corresponds to SA11 rotavirus-infected MA104 cell lysate used for molecular mass markers. Molecular masses correspond to VP4 (88 kDa), VP6 (45 kDa), and VP7 (39 kDa).

immunofluorescence results suggest that VP7$_{24}$/amy is in the ER, where most of wild-type VP7 normally is located, and does not show a markedly different or lysosomal immunofluorescence profile.

DISCUSSION

It was previously demonstrated in this laboratory and by others that the ER retention signal of VP7 resides within the first 82 NH_2-terminal residues (31, 32, 40). VP7 contains high-mannose N-linked glycosylation, at Asn-19, susceptible to Endo H digestion characteristic of ER glycoproteins (11, 14, 44). Thus, a useful marker for functional disruption of the ER retention signal is acquisition of Endo H resistance on transport to the Golgi apparatus. A deletion comprising a small part of H2 and the adjacent 11 amino acids of the mature NH_2 terminus (Δ−4–11) caused the altered molecule to enter the secretory pathway and have its carbohydrate processed by Golgi-specific enzymes (32). This suggested that NH_2-terminal residues were responsible for the retention of VP7 in the ER. The secretion of an ER protein indicates that the molecule must be folded correctly, since it has been demonstrated that misfolded proteins are retained in the ER (7, 21, 27, 34). The current studies support this view, with the added finding that some retained chimeric species are rapidly degraded (Fig. 11).

In the current studies several lines of evidence indicate that the residues Ile-9, Thr-10, and Gly-11 are essential for ER retention. Deletions were introduced into the mature NH_2 terminus of VP7 at intervals within the first 61 residues to identify the precise ER retention signal of VP7. It is clearly seen that the only deletions that resulted in secretion of VP7 were those that lacked any of the three residues Ile-9, Thr-10, and Gly-11 (Fig. 2 to 4). The fact that even subtle changes of the amino acid side chains (Ala-11 for Gly-11 and Ser-10 for Thr-10) demonstrates the absolute necessity of Ile-9, Thr-10, and Gly-11 in the ER retention of VP7. Whether they participate directly in a binding site as part of a structural motif or affect tertiary structure as might be expected from helix-breaking Gly-11 remains to be demonstrated. It is interesting that the hexapeptide LPITGS, containing the three important amino acids, is homologous to the putative targeting signal, LPSTGE, of gram-positive coccal surface proteins (37), showing that there may be some generality in the motif.

We have formally proved the retention role of this sequence by attaching it to a normally secreted protein, α-amylase, and causing the enzyme to be retained in the ER. As with VP7, deletion of any of the three amino acids resulted in secretion of the chimera.

The present study clearly demonstrated that the VP7 ER retention signal functions only when there are at least 31 mature NH_2-terminal residues of VP7 placed onto α-amylase (Fig. 8), consistent with and refining our previous conclusion that at least 61 amino acids of VP7 NH_2 terminus were needed for ER retention (31). The necessity for the chimeras to contain an additional sequence(s) beyond the Ile-9, Thr-10, and Gly-11, defined for ER retention, suggests that the residues making up the ER retention signal must be in a favorable context for function. This is apparently so in the chimeras, and porcine pancreatic α-amylase structure has been resolved to 2.9 Å (0.29 nm), which shows that the amino terminus of α-amylase seems to be on the exterior of the NH_2-terminal domain opposite the active site (4, 20). Although the exact conformation of the NH_2-terminal residues of VP7 added to α-amylase is unknown, one would expect that VP7 sequences would be exposed on the exterior of the VP7/α-amylase chimeric molecule. The loss of retention function on deletions

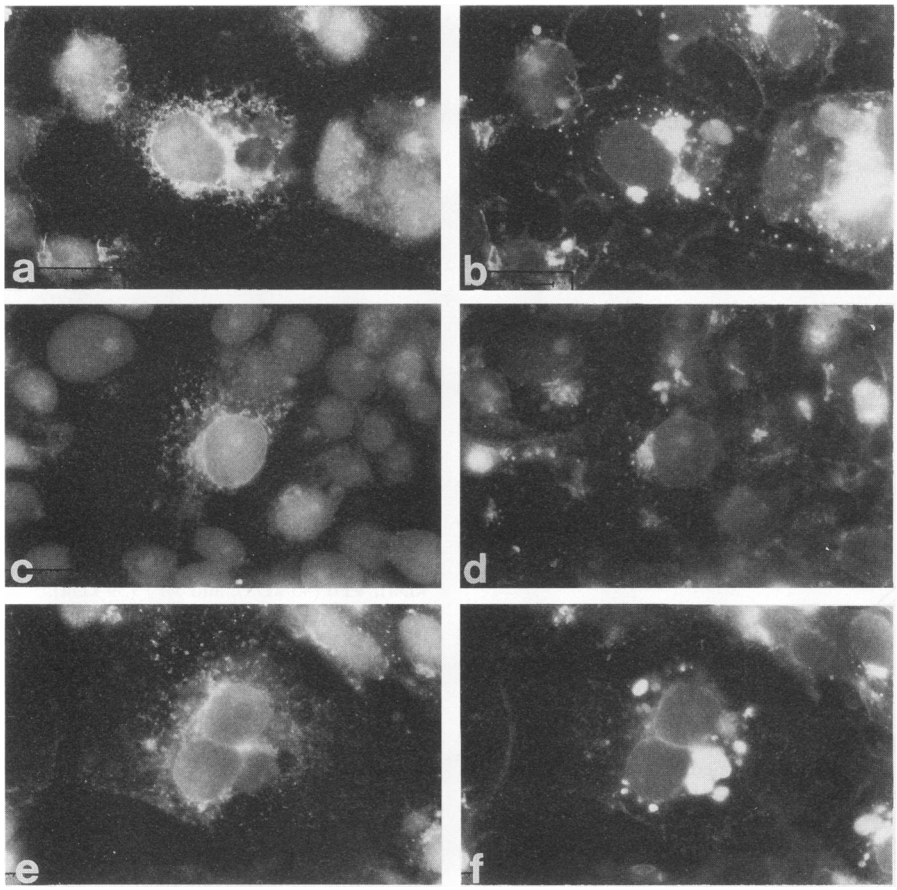

FIG. 13. $VP7_{24}$/α-amylase and $VP7_{61}$/α-amylase chimeras are localized by immunofluorescence to the ER of transfected COS7 cells. Cells were transfected with wild-type VP7 (a and b), $VP7_{61}$/amy (c and d), and $VP7_{24}$/amy (e and f), and products were detected with a polyclonal antiserum to VP7 (panel a) or α-amylase (panels c and e) and a fluorescein-conjugated secondary antibody. Cells were also double labeled with wheat germ agglutinin conjugated to rhodamine (panels b, d, and f). Magnification, ×625.

of Ile-9, Thr-10, and Gly-11 sequence in $VP7_{31}$/amy is not due to a simple shortening of the VP7 portion containing the sequence because a point mutation, $Thr\text{-}8_{31}$/amy, which does not change the length of the NH_2 terminus of VP7 resulted in secretion. The ability of Ile-9–Thr-10–Gly-11 to function within a 31-amino-acid NH_2-terminal sequence but not within a 61-amino-acid sequence (see Results) is surprising but could be related to sequences in the NH_2 terminus (residues 37 to 51) and the COOH terminus (residues 158 to 171) of VP7, which form an antigenic epitope (43). It is possible that the lack of the interacting COOH-terminal region in the larger 61-mer sequence alters the folding properties of the chimera.

It was previously observed that the ER translocation (H2) domain of VP7 was essential but not sufficient for ER retention (40). The replacement of H2 with the translocation signal sequence of influenza virus hemagglutinin resulted in the secretion of this chimera, even though it was determined that the signal was cleaved in vitro to generate the same mature molecule as wild-type VP7 (40). The role of H2 in ER retention of VP7 is unknown but may be related to the delayed ER translocation of VP7 mediated by the first 82 amino acids of VP7 (41). Attachment of H2 to a normally secreted protein, malaria S antigen, failed to retain this chimera, demonstrating the inability of H2 alone to mediate ER retention (40). Furthermore, one mutant which was secreted, Δ3–9, also retained H2 (Fig. 6). These results confirm that H2 alone is not sufficient for ER retention but further demonstrate that the prolonged presence of H2 is not sufficient for the ER retention of VP7. This also rules out the involvement of H2 as a membrane anchor, since an uncleaved variant (Δ3–9) was recovered from the medium of transfected cells (Fig. 2).

The placement of the 24 NH_2-terminal residues of VP7 resulted in a chimera retained intracellularly which did not possess α-amylase activity (Fig. 7; Table 2). This chimera was degraded rapidly, consistent with improper folding, in contrast to the long-lived, enzymatically active chimeras which were retained in the ER (Fig. 11). Degradation in the presence of chloroquine, a weak base that increases the intracellular pH and inactives lysosomal enzymes, implies that the degradation of $VP7_{24}$/amy occurs in a nonlysosomal compartment (Fig. 12). Inhibition of transport from or within the ER by incubation of cells at 16°C resulted in the inhibition of degradation of $VP7_{24}$/amy (Fig. 12). This is consistent with the transport to a post-ER/pre-Golgi compartment where the ER degradation pathway is thought to exist (5, 13). Immunofluorescence localization of $VP7_{24}$/amy revealed an ER staining pattern distinct from that of the Golgi apparatus, as was also seen for VP7 and $VP7_{61}$/amy (Fig. 13). It was previously shown in this laboratory that the processing of the VP7 carbohydrate is blocked at $Man_8GlcNAc_2$ during incubation at 15°C or in the presence of a energy inhibitor (10a, 11). It is tempting to speculate that the α-mannosidase involved in processing of the

VP7 carbohydrate to $Man_6GlcNAc_2$ and the ER degradation enzymes are located within the same compartment, which may be the salvage compartment (13).

VP7 was classified as an integral-membrane glycoprotein on the basis of its partition in the hydrophobic phase of a Triton X-114–H_2O mixture and its insolubility in sodium carbonate, although signal peptide cleavage removes the only potential transmembrane domain of VP7 (10a, 11, 42). Modeling an α-helical wheel of the first 61 amino acids of the mature NH_2 terminus forms an amphiphilic structure with distinct hydrophilic and hydrophobic faces (31). It has been previously demonstrated in this laboratory that VP7 is able to form homo-oligomers (19). It may be that the oligomerized molecule displays a completely hydrophobic exterior consistent with its membrane location. Thus, oligomerization of VP7 may be essential for the ER retention of VP7. It is also possible that such oligomerization of VP7 is altered on assembly into virus, perhaps explaining antigenic differences of viral VP7 and membrane-bound VP7 (12).

The observation that enzymatically active chimeras are retained intracellularly provides an opportunity to examine the cellular proteins which are involved in the retention of VP7 in the ER. VP7 has been transformed into yeast cells and found to be core glycosylated with no detectable Golgi modifications (unpublished observations). This implies that the VP7 retention signal is able to function in this organism. Transformation of invertase-deficient yeast cells with VP7/invertase chimeras would allow for the isolation of mutants able to grow on media with sucrose as the sole carbon source. Characterization of the gene products that are able to complement these mutants would give insight into the cellular machinery required for the ER retention of membrane-associated proteins.

The presence of a small or limited number of amino acids mediating interactions is not unknown under other circumstances such as the as the four terminal amino acids regulating the retention of several ER luminal proteins (27) or the three sequential amino acids mediating cellular binding of fibronectin (33). Although these residues are essential for the retention of VP7 in the ER, it is apparent that the conformation of this domain is also important in the functionality of this ER retention signal.

ACKNOWLEDGMENTS

We thank Robert Trimble, New York State Department of Public Health, for his gift of Endo H and Marianne Poruchynsky for her valuable suggestions.

This work was supported by National Institutes of Health grants R01-CA13402 and P01-CA13330, and D.R.M. was supported by NIH training grant CA09060.

REFERENCES

1. **Bellamy, A. R., and G. W. Both.** 1990. The molecular biology of rotavirus. Adv. Virus Res. **38:**1–43.
2. **Bernfeld, P.** 1955. Amylases α and β. Methods Enzymol. **1:**149–158.
3. **Both, G. W., J. S. Mattick, and A. R. Bellamy.** 1983. Serotype-specific glycoprotein of simian 11 rotavirus: coding assignment and gene sequence. Proc. Natl. Acad. Sci. USA **80:**3091–3095.
4. **Buisson, G., E. Diee, R. Haser, and F. Payan.** 1987. Three-dimensional structure of porcine pancreatic α-amylase at 2.9 A resolution. Role of calcium in structure and activity. EMBO J. **6:**3909–3916.
5. **Chen, C., J. S. Bonifacino, L. C. Yuan, and R. D. Klausner.** 1988. Selective degradation of T-cell antigen receptor chains retained in a pre-Golgi compartment. J. Cell Biol. **107:**2149–2162.
6. **Dahllof, B., M. Wallin, and S. Kvist.** 1991. The endoplasmic reticulum retention signal of the E3/19K protein of adenovirus-2 is microtubule binding. J. Biol. Chem. **266:**1804–1808.
7. **de Silva, A. M., W. E. Balch, and A. Helenius.** 1990. Quality control in the endoplasmic reticulum: folding and misfolding of vesicular stomatitis virus G protein in cells and in vitro. J. Cell Biol. **111:**857–866.
8. **Estes, M. K., and J. Cohen.** 1990. Rotavirus gene structure and function. Microbiol. Rev. **53:**410–449.
9. **Gluzman, Y.** 1981. SV40-transformed simian cells support the replication of early SV40 mutants. Cell **23:**175–182.
10. **Jackson, M. R., T. Nilsson, and P. A. Peterson.** 1990. Identification of a consenus motif for retention of transmembrane proteins in the endoplasmic reticulum. EMBO J. **9:**3153–3162.

10a. **Kabcenell, A.** Personal communication.

11. **Kabcenell, A. K., and P. H. Atkinson.** 1985. Processing of the rough endoplasmic reticulum membrane glycoproteins of rotavirus SA11. J. Cell Biol. **101:**1270–1280.
12. **Kabcenell, A. K., M. S. Poruchynsky, A. R. Bellamy, H. B. Greenberg, and P. H. Atkinson.** 1988. Two forms of VP7 are involved in assembly of SA11 rotavirus in endoplasmic reticulum. J. Virol. **62:**2929–2941.
13. **Klausner, R. D., and R. Sitia.** 1990. Protein degradation in the endoplasmic reticulum. Cell **62:**611–614.
14. **Kornfeld, R., and S. Kornfeld.** 1985. Assembly of asparagine-linked oligosaccharides. Ann. Rev. Biochem. **54:**631–664.
15. **Kunkel, T. A.** 1985. Rapid and efficient site-specific mutagenesis without phenotype selection. Proc. Natl. Acad. Sci. USA **82:**488–492.
16. **Laemmli, U. K.** 1970. Cleavage of structural proteins during the assembly of the head of bacteriophage T4. Nature (London) **227:**680–685.
17. **Lewis, M. J., and H. R. B. Pelham.** 1990. A human homologue of the yeast HDEL receptor. Nature (London) **348:**162–163.
18. **Lewis, M. J., D. J. Sweet, and H. R. B. Pelham.** 1990. The ERD2 gene determines the specificity of the luminal ER protein retention system. Cell **61:**1359–1363.
19. **Maass, D. R., and P. H. Atkinson.** 1990. Rotavirus proteins VP7, NS28, and VP4 form oligomeric structures. J. Virol. **64:**2632–2641.
20. **MacGregor, E. A., and B. Svensson.** 1989. A super-secondary structure predicted to be common to several α-1,4-D-glucan-cleaving enzymes. Biochem. J. **259:**145–152.
21. **Machamer, C. E., R. W. Doms, D. G. Bole, A. Helenius, and J. K. Rose.** 1990. Heavy chain binding protein recognizes incompletely disulfide-bonded forms of vesicular stomatitis virus G protein. J. Biol. Chem. **265:**6879–6883.
22. **Maniatis, T., E. Fritsch, and J. Sambrook.** 1982. Molecular cloning: a laboratory manual. Cold Spring Harbor Laboratory, Cold Spring Harbor, N.Y.
23. **Munro, S., and H. R. B. Pelham.** 1987. A C-terminal signal prevents secretion of luminal ER proteins. Cell **48:**899–907.
24. **Nilsson, T., M. Jackson, and P. A. Peterson.** 1989. Short cytoplasmic sequences serve as retention signals for transmembrane proteins in the endoplasmic reticulum. Cell **58:**707–718.
25. **Ohkuma, S., and B. Poole.** 1978. Fluorescence probe measurement of the intralysosomal pH and the perturbation of pH by various agents. Proc. Natl. Acad. Sci. USA **75:**3327–3331.
26. **Paabo, S., B. M. Bhat, S. M. Wold, and P. A. Peterson.** 1987. A short sequence in the COOH-terminus makes an adenovirus membrane glycoprotein a resident of the endoplasmic reticulum. Cell **50:**311–317.
27. **Pelham, H. R. B.** 1989. Control of protein exit from the endoplasmic reticulum. Annu. Rev. Cell Biol. **5:**1–23.
28. **Pelham, H. R. B., K. G. Hardwick, and M. J. Lewis.** 1988. Sorting of soluble ER proteins in yeast. EMBO J. **7:**1757–1762.
29. **Pelham, H. R. B., and R. J. Jackson.** 1976. An efficient mRNA-dependent translation system from reticulocyte lysates. Eur. J. Biochem. **67:**242–256.
30. **Petrie, B. L., H. B. Greenberg, D. Y. Graham, and M. K. Estes.** 1984. Ultrastructural localization of rotavirus antigens using colloidal gold. Virus Res. **1:**133–152.
31. **Poruchynsky, M. S., and P. H. Atkinson.** 1988. Primary sequence domains required for the retention of rotavirus VP7 in the endoplasmic reticulum. J. Cell Biol. **107:**1697–1706.
32. **Poruchynsky, M. S., C. Tyndall, G. W. Both, F. Sato, A. R. Bellamy, and P. H. Atkinson.** 1985. Deletions into an NH_2-

terminal hydophobic domain result in secretion of rotavirus VP7, a resident endoplasmic reticulum membrane glycoprotein. J. Cell Biol. **101:**2199–2209.

33. **Pytela, R., M. D. Pierschbacher, S. Argraves, S. Suzuki, and E. Ruoslahti.** 1987. Arginine-glycine-aspartic acid adhesion receptors. Methods Enzymol. **144:**475–489.
34. **Rose, J. K., and R. W. Doms.** 1988. Regulation of protein export from the endoplasmic reticulum. Annu. Rev. Cell Biol. **4:**257–288.
35. **Sanger, F., S. Nicklen, and A. R. Coulson.** 1977. DNA sequencing with chain-terminating inhibitors. Proc. Natl. Acad. Sci. USA **74:**5463–5467.
36. **Saraste, J., and E. Kuismanen.** 1984. Pre- and post-Golgi vacuoles operate in the transport of Semliki Forest virus membrane glycoproteins to the cell surface. Cell **38:**535–549.
37. **Scheewind, O., K. F. Jones, and V. A. Fishchetti.** 1990. Sequence and structural characteristics of the trypsin-resistant surface protein of group A streptococci. J. Bacteriol. **172:**3310–3317.
38. **Semenza, J. C., K. G. Hardwick, N. Dean, and H. R. B. Pelham.** 1990. ERD2, a yeast gene required for the receptor-mediated retrieval of luminal ER proteins from the secretory pathway. Cell **61:**1349–1357.
39. **Shields, D., and G. Blobel.** 1978. Efficient cleavage and segregation of nascent presecretory proteins in a reticulocyte lysate supplemented with microsomal membranes. J. Biol. Chem. **253:**3753–3756.
40. **Stirzaker, S. C., and G. W. Both.** 1989. The signal peptide of the rotavirus glycoprotein VP7 is essential for its retention in the endoplasmic reticulum as an integral membrane protein. Cell **56:**741–747.
41. **Stirzaker, S. C., D. Poncet, and G. W. Both.** 1990. Sequences in the rotavirus glycoprotein VP7 which mediates delayed translocation and retention of the protein in the ER. J. Cell Biol. **111:**1343–1350.
42. **Stirazaker, S. C., P. L. Whitfeld, D. L. Christie, A. R. Bellamy, and G. W. Both.** 1987. Processing of rotavirus glycoprotein VP7: implications for the retention of the protein in the endoplasmic reticulum. J. Cell Biol. **105:**2897–2903.
43. **Taniguchi, K., Y. Hoshino, K. Nishikawa, K. Y. Green, W. L. Maloy, Y. Morita, S. Urasawa, A. Z. Kapikian, R. M. Chanock, and M. Gorziglia.** 1988. Cross-reactive and serotype-specific neutralization epitopes on VP7 in human rotavirus: nucleotide sequence analysis of antigenic mutants selected with monoclonal antibodies. J. Virol. **62:**1870–1874.
44. **Tarentino, A. L., and F. Maley.** 1974. Purification and properties of an endo-N-acetylglucosaminidase from Streptomyces griseus. J. Biol. Chem. **249:**811–817.
45. **Tartakoff, A. M.** 1986. Temperature and energy dependence of secretory protein transport in the exocrine pancreas. EMBO J. **5:**1477–1482.
46. **Tartakoff, A. M., and P. Vassalli.** 1983. Lectin-binding sites as markers of Golgi subcompartments: proximal-to-distal maturation of oligosaccharides. J. Cell Biol. **97:**1243–1248.
47. **Tkacz, J. S., and J. O. Lampen.** 1975. Tunicamycin inhibition of polyisoprenyl N-acetylglucosaminyl pyrophosphate formation in calf liver microsomes. Biochem. Biophys. Res. Commun. **65:**245–257.
48. **Vaux, D., J. Tooze, and S. Fuller.** 1990. Identification by anti-idiotypic antibodies of an intracellular membrane protein that recognizes a mammalian endoplasmic reticulum retention signal. Nature (London) **345:**495–502.
49. **Whitfeld, P. L., C. Tyndall, S. C. Stirzaker, A. R. Bellamy, and G. W. Both.** 1987. Location of signal sequences within the rotavirus SA11 glycoprotein VP7 which direct it to the endoplasmic reticulum. Mol. Cell. Biol. **7:**2491–2497.
50. **Wibo, M., and B. Poole.** 1974. Protein degradation in cultured cells. II. The uptake of chloroquine by rat fibroblasts and the inhibition of cellular protein degradation and cathepsin B_1. J. Cell Biol. **63:**430–440.
51. **Zagouras, P., and J. K. Rose.** 1989. Carboxy-terminal SEKDEL sequences retard but do not retain two secretory proteins in the endoplasmic reticulum. J. Cell Biol. **109:**2633–2640.
52. **Zoller, M. J., and M. Smith.** 1982. Oligonucleotide-directed mutagenesis: a simple method using two primers and a single-stranded DNA template. Nucleic Acids Res. **10:**6487–6500.